The anti-angiogenic effect of Astragalus hamosus extract on human umbilical vein endothelial cells cultured on three-dimensional fibrin gel model

Jafar Ai
Tehran University of Medical Sciences
Saeed Samani
Tehran University of Medical Sciences
Maria Kavianpour
Tehran University of Medical Sciences
Somayeh Ebrahimi-Barough
Tehran University of Medical Sciences
Mohammad Abdi
Kurdistan University of Medical Sciences
Elmira Mikaeiliagah
West Virginia University
Naghmeh Bahrami
Tehran University of Medical Sciences
Rezgar Rahbari
Kurdistan University of Medical Sciences
Armin Ai
Tehran University of Medical Sciences
Mozaffar Mahmoodi (m.mahmoodi@muk.ac.ir)
Kurdistan University of Medical Sciences

Article

Keywords: Astragalus hamosus, Angiogenesis, Apoptosis, Paclitaxel.

Posted Date: August 25th, 2022

DOI: https://doi.org/10.21203/rs.3.rs-1960472/v1

Abstract

Objective: Angiogenesis is necessary for solid tumors to grow and metastasize because it provides oxygen and nutrients for the tumor. By considering similar anti-tumor activity by a similar mechanism in herbal medicine, Astragalus hamosus (A. hamosus) was used in this study in a 3D fibrin gel model against human umbilical vein endothelial cells (HUVECs) to investigate its anti-angiogenic properties.

Materials and Methods: A. hamosus extract was tested for cytotoxicity on HUVECs using MTT assay. Flow cytometry was used to examine apoptosis, cell cycle, and proliferation. Also, by qPCR, we quantified the expression of genes related to apoptosis, such as caspase-9, -8, -3, and Bcl-2.

Results: Angiogenic activities of HUVECs were significantly decreased after treatment with IC50 concentration of A. hamosus extract. Flow cytometry analysis revealed that the cell cycle in HUVECs was arrested in G0/G1 phase in the 3D model higher than 2D culture. Anti-proliferation activity of the extract decreased the expression of Ki-67, especially in the 3D culture.

Conclusion: Based on our results, A. hamosus extract can be used to treat tumors by inhibiting angiogenesis. Also, 3D fibrin gel can simulate anti-proliferative and anti-apoptotic properties of tumors better than 2D culture environment.

1. Introduction

Sprouting angiogenesis is the formation of new blood vessels from pre-existing ones [1], and physiologically plays many roles in different healthy and pathological processes including tumor growth and metastasis [2]. In solid tumors, such as breast cancer angiogenesis provides additional nutrients and potential pathways for tumor spreading and is the main reason for the poor prognosis of cancer patients [3]. Today, many studies are attempting to identify factors promoting and supporting angiogenesis to prevent tumor growth and metastasis [4, 5].

Paclitaxel (PTX) is a cancer chemotherapy drug that is widely used as a first-line treatment for many common malignancies. It also has high antitumor activity against some rare malignancies such as angiosarcoma and Kaposi's sarcoma. Paclitaxel belongs to the taxane class of drugs and was the first taxane to enter clinical trials and be approved by the FDA. Paclitaxel binds to the beta subunit of polymerized tubulin and inhibits the rate of dissociation of the tubulin subunits from the tubule. Thus, micromolar administration of paclitaxel to cells leads to the formation of microtubule bundles and asters that arrest the cells in mitosis [6]. Paclitaxel has significant anti-angiogenic activity attributed to cytotoxic and cytostatic activity on activated endothelial cells or inhibition of capillary formation and cell migration. In addition, paclitaxel has been shown to inhibit VEGF and Ang-1 release by tumor cells and increase thrombospondin-1 (TSP-1) secretion into the tumor microenvironment [6].

Considering damages to normal cells caused by anti-cancer chemotherapy drugs, significant efforts have been made to identify natural compounds and related synthetic agents to prevent cancer development

and recurrence [7]. Traditional herbal medicine has a long history of clinical use in cancer and treatment of various diseases in Asia [7]. Increasing evidence has shown potential proangiogenic benefits of herbal medicines, while tumor angiogenesis may be inhibited by the active components [8, 9]. For example, anti-angiogenic activity has been identified for Cimicifuga foetida, Rehmannia glutinosa, and Albatrellus confluens via different pathways [10].

Furthermore, some traditional medicinal compounds have been effective in treating painful and inflammatory conditions in many animal models, including Astragalus hamosus (*A. hamosus*) [11]. Pharmacological studies have shown the antioxidant activity of the methanolic extract of *A. hamosus* [12] whose volatile compounds have significant cytotoxic activity against human acute lymphocytic leukemia in a concentration-dependent manner [13]. Evaluation of the antiproliferative effect of the methanolic extract of *A. hamosus* have showed a concentration-dependent inhibition of malignant cell proliferation [14]. The flavonoids derived from this plant can improve the treatment of hepatocellular carcinoma in rats. The results suggest that it prevents hepatocellular carcinoma by suppressing the increase in serum marker enzyme levels and free radicals [15]. The results of a meta-analysis of randomized studies also showed that astragalus-based herbal medicine could increase the effectiveness of cancer treatment when combined with chemotherapy [16]. To address these issues, researchers in the field of cancer research are now using three-dimensional (3D) culture models, which has enabled researchers to design systems that capture the physiological cell-cell and cell-ECM interactions of a variety of tissue types [17]. Hydrogels are used as hydrophilic polymeric networks to create 3D *in vitro* models of tissues. A variety of natural and synthetic hydrogel materials have been employed to create engineered 3D tumor microenvironments supporting cancer cell growth and angiogenesis, and providing mechanical and chemical supports to regulate tumor behavior within the matrix [18]. Fibrinogen is a large glycoprotein found in plasma that plays a critical role in blood coagulation, fibrinolysis, cell and matrix interactions, the inflammatory response, wound healing, and neoplasia [19]. Fibrin hydrogels are widely used as an artificial microenvironment as they have a nano/macro fibrous architecture that mimics the native ECMs [20].

In our previous article [20], we extracted A. hamosus, identified its total steroids, calculated its IC50 value against MCF-7 breast cancer cell line, and developed a 3D fibrin gel model to show the better inhibitory effect of A. hamosus extract on encapsulated evaluate MCF-7 spheroids. In this study, the inhibitory effect of A. hamosus fruit extract on angiogenesis in a three-dimensional (3D) model of breast cancer was determined and compared to paclitaxel (PTX).

2. Materials And Methods

2.1. Preparation of *A. hamosus* extract

Preparation and characterization of *A. hamosus* extract was introduced in our previous article [20]. Briefly, the fruit of *A. hamosus* plant (voucher specimen number of PMP-3610 assigned by Herbarium of Pharmacy of Tehran University of Medical Sciences) was massaged in 70% ethanol, filtered, concentrated

in vacuum evaporator, and the dried extract was suspended in deionized water to yield different fractions. The total steroids (amount of steroids and cholesterol) in the weight percent in *A. hamosus* was determined by the Lieberman-Bouchard test, and recorded as 0.166%(w/w). The necessary permits to collect and use the facility have been obtained. Furthermore, all plant experiments complied with the relevant institutional, national and international guidelines and laws.

2.2. Cells Culture

Human umbilical vein endothelial cells (HUVECs) were purchased from the Cell Bank of the Pasteur Institute of Iran (Tehran, Iran). They were cultured in Dulbecco's modified Eagle's medium (DMEM) and RPMI-1640 medium supplemented with 10% fetal bovine serum (FBS) and 1% penicillin-streptomycin (all from Gibco). The cells were maintained under common conditions (37°C, 95% humidity, and 5% CO_2), cell culture mediums were changed every 2–3 days, and the cells were passaged after reaching 65–80% confluent.

2.3. Determination of IC_{50} concentrations by MTT assay

The HUVECs at a density of 5000 cells/well were cultivated in 96-well plates, and incubated under common cell culture conditions for 24 hours. Then Concentrations of 62.5, 125, 250, and 500 µg/mL for *A. hamosus* and concentrations of 0.005, 0.01, 0.05, and 0.1 µmol/mL for PTX were prepared and examined separately to calculate IC_{50} (inhibition concentration). After 72 hours, the supernatants were replaced by MTT solution (0.5 mg/mL in phosphate-buffered saline) and incubated for four hours at 37°C. After discarding the supernatant, the formazan crystals were dissolved by 150 µL DMSO (Sigma-Aldrich), and light absorption was measured at 570 nm using an EL340 microplate reader (BioTek, USA) to calculate IC_{50} concentrations.

2.4. Three-Dimensional in vitro tumor angiogenesis assays

2.4.1. Tube Formation assay for *in vitro* Angiogenesis

In our previous published article [20], we analyzed different compositions of fibrin gels to make a 3D model having viscoelastic properties closer to natural breast cancer tissue. According to our findings, following composition was acceptable for a suitable 3D fibrin gel model: 6 mg fibrinogen in 1 mL M199 solution, 30 µL of thrombin (120 U/ml in 1 M sodium buffer), 45 µL of calcium chloride ($CaCl_2$, 1% (w/v)), and 15 µL of fetal bovine serum (FBS). To form a 3D fibrin model, fibrinogen solution is transferred to a culture plate, other components are added, and the mixture is incubated at 37 ºC for one hour.

Angiogenic activities of HUVECs were stimulated with a starving medium (a medium without growth factors or FBS) for 24 hours prior to performing the tube formation assay in complete culture medium (High glucose DMEM + 10%FBS + 1% antibiotics). After dislodging HUVECs from the surface of the flask using tyrosinase and making 3D fibrin gel model (200 µL/well in 96-well plate), dissociated HUVECs (2×10^5 cell/mL) were re-suspended in complete culture medium, and 100 µL of cell suspension was add to each well. By forming a vascular network after 24 hours, the samples were separately treated with IC_{50}

concentrations of *A. hamosus* extract and PTX for 72 hours. Finally, the effect of each treatment on the vascular network was investigated using an Olympus BX61 phase-contrast microscope (Olympus Corporation, Japan).

2.4.2. Flow cytometry analysis of the cell cycle, cell proliferation, and apoptosis

After 72-hours treatment of HUVECs by IC_{50} concentrations of *A. hamosus* extract and PTX in the 6-well plate, the supernatant was collected, adherent cells were detached by brief trypsinization, and transferred to their collected supernatants. Then, harvested cells were rinsed with ice-cold PBS, and re-suspended in 500 µL of 70% ethanol overnight to synchronize the cell cycle. Following this, the cells were centrifuged at 2000 rpm for five minutes, re-suspended in 500 µL of PBS containing 50 µg RNase A (0.1 µg/mL) and Propidium Iodide (PI, 0.01 µg/mL), incubated in darkness at 25°C for 30 minutes, and analyzed for the cell cycle. The DNA content was determined by a FACS Caliber flow cytometer (CyFlow SL, Partec, Germany) and the cells were analyzed in different phases of G0, G1, S, and M. All experiments were performed in triplicates.

For cell proliferation analysis, after 72 hours, the cells were fixed with 4% paraformaldehyde for 10 minutes at 25°C, and in 70% ethanol. Then, the cells were suspended in cold PBS containing FITC-labeled anti-Ki-67 antibody (BD Biosciences, USA), and incubated at 4°C for 30 minutes. Treated cells were then washed with PBS and centrifuged to remove non-reacted fluorophore molecules.

Annexin V-PI assay was used to detect the percentage of HUVECs in the apoptosis phase. After 72 hours treatment of HUVECs by IC_{50} concentrations of *A. hamosus* extract and PTX, the Annexin V and PI reagents were added to harvest HUVECs, and kept in the dark on ice for 30 minutes. Then, the cells were washed with PBS and subjected to flow cytometry techniques. The fluorescence of the labeled cells was measured using a flow cytometer (FACS Calibur, Becton Dickinson, San Jose, CA) and data was analyzed by FlowJo software.

2.4.3. Quantitative real time-PCR (qPCR) for apoptosis analysis

The qPCR analysis was performed to evaluate the expression of initiative and executive apoptosis genes. For this, trizol solution (Invitrogen, USA) was used to extract total RNA from HUVEC-seeded fibrin gels treated with the IC_{50} concentrations of PTX and A. hamosus extract according to the manufacturer's instructions. After synthesis of complementary DNA (cDNA) using the First Strand cDNA Synthesis kit (Takara, Korea), the expressions of Caspase-9, Caspase-8, Caspase-3, Bcl-2, and β-globin as housekeeping genes were analyzed by qPCR using a SYBR-Green kit (Takara, Korea) and the Step One Real-Time PCR System (Applied Biosystems, USA). Table 1 includes the forward and reverse sequences for mentioned genes. All Ct values calculated from the target genes were normalized to the β-globin gene, and the comparative Ct method, $2^{-\Delta\Delta Ct}$, was used for relative gene expression analysis.

Table 1
Primers used for Quantitative RT-PCR

Gene	Accession No.	Primer sequence (5'◊3')	Size (bp)	Annealing(°C)
Caspase 9	NM_001278054.2	**F**: GTTTGAGGACCTTCGACCAGCT	129	62
		R: CAACGTACCAGGAGCCACTCTT		
Caspase 8	NM_001372051.1	**F**: GAAGAGGGTCATCCTGGGAGA	142	61
		R: TCAGGACTTCCTTCAAGGCTGC		
Caspase 3	NM_001354783.2	**F**: GGAAGCGAATCAATGGACTCTGG	146	61
		R: GCATCGACATCTGTACCAGACC		
BCL2	NM_000633.3	**F**: ATCGCCCTGTGGATGACTGAGT	127	62
		R:GCCAGGAGAAATCAAACAGAGGC		
β-globin	NM_000518	**F**: CACCTTTGCCACACTGAGTGAG	1002	61
		R: CCACTTTCTGATAGGCAGCCTG		

2.5. Statistical analysis

All experiments were performed in three independent experiments and data was reported as mean ± standard deviation (SD). Statistical comparisons were carried out using one-way analysis of variance (ANOVA) followed by Tukey's post hoc test at significance level of 0.05.

3. Results

3.1. IC_{50} concentrations of *A. hamosus* extract and PTX on HUVEC cell line

To optimize the concentration of *A. hamosus* extract and PTX to be used in further experiments, the IC_{50} value was calculated on the HUVEC for 72 hours. By considering the non-treated cells as control groups, normalized absorbance against *A. hamosus* extract and PTX concentration was plotted to calculate the IC_{50} values by curve fitting on the MTT data. The MTT results (Fig. 1) showed that *A. hamosus* extract and PTX decreased the cell viability of HUVECs by increasing the concentration of treating agents. According to Fig. 1, the IC_{50} values of *A. hamosus* extract and PTX were 533.7 µgr/mL and 0.012 µM/mL, respectively.

3.2. Anti-angiogenesis effect of *A. hamosus* extract against vascular tube formation

After seeding HUVECs on the top of the fibrin gel, the cells began to sprout and form short, narrow cord-like structures in 1–2 days (Fig. 2A), while treatment by PTX and *A. hamosus* extract caused disruption of

the capillary tube network compared to untreated controls (Fig. 2B **and C**). To investigate the effect of *A. hamosus* extract on angiogenesis *in vitro*, the length of the tubes was examined after 72 hours (Fig. 2D). PTX and *A. hamosus* at their IC_{50} concentrations significantly prevented tube formation among which PTX had the highest effect.

3.3. Cell cycle phases in HUVEC cells

To investigate the suppression effects of *A. hamosus* and PTX on cell proliferation through cell cycle arrest, the HUVECs were treated at IC_{50} concentrations in 2D and 3D cultures, and the cell cycle distribution was analyzed by flow cytometry. Figure 3 shows obvious changes in percentages of cell cycle phases, the histograms, and the percentage of cells in each cell cycle phase categorized into G1/G0, S, and G2/M phases. *A. hamosus* extract and PTX could stimulate arrest in G0/G1 phase, and the percentage of G0/G1 phase in 2D and 3D cultures significantly decreased compared to the control group. In contrast, *A. hamosus* extract and PTX caused an increase in the S and G2/M phases in both 2D and 3D environments.

3.4. Anti-proliferative effect of *A. hamosus* on HUVEC cells

The proliferation rate of HUVEC cells treated with *A. hamosus* and PTX at IC_{50} concentrations under 2D and 3D culture conditions was determined by analysis of Ki-67 expression. As shown in Fig. 4, the Ki-67 expression decreased significantly in treated HUVECs, especially in 3D cultured cells, compared to the control groups. Despite greater influence of 3D culture condition on anti-proliferative abilities of both agents, the Ki67 expression in the PTX-treated HUVECs was lower than that of the *A. hamosus*-treated cells.

3.5. Apoptosis induction in HUVECs

The apoptosis index of the HUVECs-treated with *A. hamosus* and PTX at their IC_{50} concentrations was analyzed with Annexin V-PI by flow cytometry (Fig. 5I). The control group possessed the lowest level of apoptosis who's total 2D and 3D apoptosis were 21.9% (3.1% early and 18.8% late apoptosis) and 7.88% (1.93% early and 5.95% late apoptosis), respectively (Fig. 5II). In both 2D and 3D culture models, PTX treatment caused a significant increase in apoptosis and decrease in cell viability compared to *A. hamosus* group.

Further, apoptotic genes (caspase-9, caspase-8, caspase-3, and anti-apoptotic protein expression Bcl-2) were examined in HUVECs. Real time-PCR results (Fig. 6) showed that the expressions of Casp9, Casp8, and Casp3 in PTX-treated HUVECs were significantly higher than those in *A. hamosus*-treated cells in 2D culture model. Although most genes were upregulated significantly in the 3D culture model compared to the 2D model, the expression levels of Casp9 and Casp3 were higher in PTX-treated HUVECs.

4. Discussion

Angiogenesis is one of the most important processes that provides sufficient nutrients and oxygen for tumor cells, and plays an important role in metastasis induction and cancer progression [2]. In this study, we analyzed the anti-angiogenic effect of the fruit extraction of *A. hamosus* in a 3D fibrin gel, and compared it with the effects of PTX. To do that, the IC_{50} doses of the *A. hamosus* and PTX were determined, cell cycle, proliferation, and apoptosis of HUVECs were studied at IC_{50} concentrations.

Treatment of HUVECs with *A. hamosus* extract in the 3D fibrin gel caused incomplete tubular structure having significantly fewer branch points and shorter tube lengths compared to the untreated control group. Further, the results demonstrated that *A. hamosus* could suppress cell proliferation through cell cycle arrest in both 2D and 3D models. Despite lower G0/G1 and higher S and G2/M in the *A. hamosus*- and PTX-treated groups than those of control group, the 3D fibrin model had a significant effect on the G0/G1 arrest in the *A. hamosus*-treated HUVECs compared to the PTX-treated one. Also, the expression of Ki-67 as the marker of cell proliferation decreased, especially in 3D cultured cells compared to the control groups. Flow cytometry and qRT analyses confirmed that *A. hamosus* treatment increased apoptosis and decreased cell viability both 2D and 3D culture models. Late apoptosis in the 3D model was significantly higher than that of 2D model, while early apoptosis was significantly lower in the 3D model than in 2D one. Based on qPCR analysis, the expression levels of caspase-9, -8, and − 3 were higher in the *A. hamosus*- and PTX-treated HUVECs compared to untreated cells. After treatments with *A. hamosus* or PTX, caspase-8 increased more in the 3D culture model than the 2D group. Although the expression level of Bcl-2 increased in the 3D culture model, its expression was not significant for both treatment groups.

Various studies have been reported on the effects of *A. hamosus* plant so far. In traditional medicine, *A. hamosus* extract has been prescribed to treat inflammation-related diseases because of its antioxidant and anti-inflammatory activities [3, 21]. For example, Braga et al. found that the antioxidant activity of extract of *A. hamosus* leaves can interfere with reactive oxygen/nitrogen species (ROS/RNS). These findings are interesting for improving the antioxidant network, restoring redox balance in human neutrophil cells, and extending the possibility of using plant-derived molecules to antagonize the generated oxidative stresses in living organisms [4]. Also, some in vivo studies have shown the anti-inflammatory activity of *A. hamosus* on acute inflammations [22]. Ansari et al. examined the *A. hamosus* oil on osteoarthritis, and demonstrated that this oil could relieve the pain in older people with mild to moderate knee osteoarthritis [8].

Many recent active screening studies have found that ingredients of Astragalus such as polysaccharides, saponins, and flavonoids have anti-tumor properties. In a study conducted by Tian et al., they investigated the adjunct cancer-fighting effect of Astragalus polysaccharides on H22 tumor-bearing mice. They found a synergistic anti-tumor effect between Astragalus polysaccharides and adriamycin which alleviated the consequences of adriamycin on the spleen and thymus in H22 tumor-bearing mice [9]. It has been demonstrated that astragaloside IV can reduce the expression of Vav3.1 in a dose- and time-dependent manner. The Vav3.1 is highly expressed in ovarian cancer stem cells and is clinically relevant for prognosis prediction [10]. The researchers also found that astragaloside II could exert multidrug resistance reversal effects and adjuncts to hepatic cancer chemotherapy [11]. Experimental data showed

that Astragalus flavonoids could inhibit the proliferation of K562 myelogenous leukemia cells [12]. Further, a comparison of the anti-tumor activity of the isolated mixture of two *A. hamosu*-derived saponins with some chemotherapy drugs such as dinaline, decitabine, erufosine, and tamoxifen in two breast cancer cell lines confirmed the anti-neoplastic activity of the saponin mixture [13].

5. Conclusion

In this study, we talked about the importance of anti-angiogenesis to control cancer progression, and evaluated the effect of *A. hamosus* extract on proliferation and tube formation of HUVECs.

Fibrin gel as a suitable 3D microenvironment had a viscoelasticity behavior close to natural breast tissue, and could improve the apoptotic performance of *A. hamosus*. The hydroalcoholic extract of *A. hamosus* significantly reduced the survival of HUVECs in the 3D fibrin gel model compared to the 2D culture indicating the apoptotic activity of steroid compounds in *A. hamosus*. Examining caspase activation in both 2D and 3D culture models showed that the *A. hamosus* exerted its apoptotic effects in the internal pathway of apoptosis (i.e. caspase-9), and this effect was especially distinct in 3D fibrin gel. In addition, this extract significantly reduced the cell proliferation of HUVEC in 3D culture environment compared to 2D culture confirming the positive effect of 3D condition on intensifying the antiproliferative effect of *A. hamosus*. In this study, the anti-angiogenic effect of the *A. hamosus* and its effect on cell cycle arrest in fibrin gel was clearly observed and well demonstrated in comparison with 2D culture. In conclusion, fibrin gel can serve as a suitable scaffold to evaluate drug response in the cancer study. Our data indicate that the *in vitro* use of herbal medicine may have an anti-angiogenic effect on cells involved in angiogenesis; however, the mechanisms of *A. hamosus* anti-angiogenic and anti-proliferative activities are still unclear, and through what exact signaling pathway it exerts these effects. Further investigation is needed to determine its anti-neoplastic potential.

Declarations

Funding details

This work was supported by the Tehran University of Medical Sciences under
Grant IR.TUMS.VCR.REC.1397.980.

Disclosure statement

No potential conflict of interest was reported by the author(s).

Availability of data and material

The datasets used and/or analyzed during the current study are available from the corresponding author upon reasonable request.

Authors' contributions

Conceptualization: [Mozaffar Mahmoodi] and [Jafar Ai]; Methodology: [Somayeh Ebrahimi-Barough], [Elmira Mikaeiliagah], [Naghmeh Bahrami], [Armin Ai], and [Mozaffar Mahmoodi]; Formal analysis and investigation: [Mozaffar Mahmoodi], [Rezgar Rahbari], [Mohammd Abdi], and [Somayeh Ebrahimi-Barough]; Writing-original draft preparation: [Mozaffar Mahmoodi], [Saeed Samani], [Maria Kavianpour]; Writing-review and editing: [Mozaffar Mahmoodi]; Funding acquisition: [Jafar Ai]; Resources: [Jafar Ai], [Mohammd Abdi]; Supervision: [Jafar Ai]. The authors read and approved the final manuscript.

Acknowledgements

The authors wish to thank Tehran University of Medical Sciences. The authors would like to appreciate the Kurdistan University of Medical Sciences for the partial support of this research.

References

1. M. Mahmoodi, S. Ferdowsi, S. Ebrahimi-Barough, S. Kamian, and J. Ai, "Tissue engineering applications in breast cancer," Journal of Medical Engineering and Technology. **vol**. **44**, no. 4, pp. 162 – 16).2020(.
2. C. Wei et al., "Crosstalk between cancer cells and tumor associated macrophages is required for mesenchymal circulating tumor cell-mediated colorectal cancer metastasis," Molecular Cancer. **vol**. **18**, no. 1(2019).
3. L. Pleşca-Manea, A. E. Pârvu, M. Pârvu, M. Taămaş, R. Buia, and M. Puia, "Effects of Melilotus officinalis on acute inflammation," Phytotherapy Research. **vol**. **16**, no. 4, pp. 316–319(2002).
4. P. C. Braga et al., "Antioxidant activity of calendula officinalis extract: Inhibitory effects on chemiluminescence of human neutrophil bursts and electron paramagnetic resonance spectroscopy," Pharmacology. **vol**. **83**, no. 6, pp. 348–355(2009).
5. R. Narimani, A. Tarakemeh, M. Moghaddam, and M. Mahmoodi Sourestani, "Phytochemical Variation within Aerial Parts of Ferula cupularis Populations, an Endangered Medicinal Plant from Iran," Chemistry and Biodiversity. **vol**. **18**, no. 12(2021).
6. G. Bocci, A. Di Paolo, and R. Danesi, "The pharmacological bases of the antiangiogenic activity of paclitaxel," Angiogenesis. **vol**. **16**, no. 3, pp. 481–492(2013).
7. M. Greenwell and P. K. S. M. Rahman, "Medicinal Plants: Their Use in Anticancer Treatment," International journal of pharmaceutical sciences and research. **vol**. **6**, no. 10, pp. 4103–4112(2015).
8. G. Ansari et al., "The effect of Melilotous Officinalis oil on the physical function of older adults with mild to moderate knee osteoarthritis: A double-blind randomized controlled trial," Iranian Journal of Ageing. **vol**. **14**, no. 2, pp. 132–143(2019).
9. Q. E. Tian, H. D. Li, M. Yan, H. L. Cai, Q. Y. Tan, and W. Y. Zhang, "Astragalus polysaccharides can regulate cytokine and P-glycoprotein expression in H22 tumor-bearing mice," World Journal of Gastroenterology. **vol**. **18**, no. 47, pp. 7079–7086(2012).

10. H. Qi, L. Wei, Y. Han, Q. Zhang, A. S.-Y. Lau, and J. Rong, "Proteomic characterization of the cellular response to chemopreventive triterpenoid astragaloside IV in human hepatocellular carcinoma cell line HepG2," International Journal of Oncology. **vol**. **36**, no. 3, pp. 725–735(2010).
11. C. Huang, D. Xu, Q. Xia, P. Wang, C. Rong, and Y. Su, "Reversal of P-glycoprotein-mediated multidrug resistance of human hepatic cancer cells by Astragaloside II," Journal of Pharmacy and Pharmacology. **vol**. **64**, no. 12, pp. 1741–1750(2012).
12. D. Zhang et al., "Investigation of effects and mechanisms of total flavonoids of astragalus and calycosin on human erythroleukemia cells," Oxidative Medicine and Cellular Longevity. **vol**. **5**, no. 11, pp. 851–861(2012).
13. K. Umer, F. Zeenat, W. Ahmad, and A. Khan, "Therapeutics, phytochemistry and pharmacology of Iklilul Malik (Astragalus hamosus Linn): A Natural Unani Remedy," International Journal of Herbal Medicine. **vol**. **5**, no. 5, pp. 1–5(2017).
14. I. Krasteva, G. Momekov, P. Zdraveva, S. Konstantinov, and S. Nikolov, "Antiproliferative effects of a flavonoid and saponins from Astragalus hamosus against human tumor cell lines," Pharmacognosy Magazine. **vol**. **4**, no. 16, pp. 269–272(2008).
15. S. Saleem et al., "Anticancer potential of rhamnocitrin 4'-β-d-galactopyranoside against N-diethylnitrosamine-induced hepatocellular carcinoma in rats," Molecular and Cellular Biochemistry. **vol**. **38**, no. 1–2, pp. 147–153(2013).
16. M. McCulloch et al., "Astragalus-based Chinese herbs and platinum-based chemotherapy for advanced non-small-cell lung cancer: Meta-analysis of randomized trials," Journal of Clinical Oncology. **vol**. **24**, no. 3, pp. 419–430(2006).
17. M. Song et al., "MiR-139-5p inhibits migration and invasion of colorectal cancer by downregulating AMFR and NOTCH1," Protein and Cell. **vol**. **5**, no. 11, pp. 851–861(2014).
18. W. Chen, Y. Yuan, C. Li, H. Mao, B. Liu, and X. Jiang, "Modulating Tumor Extracellular Matrix by Simultaneous Inhibition of Two Cancer Cell Receptors," Advanced Materials. **vol**. **34**, no. 10(2022).
19. M. W. Mosesson, "Fibrinogen and fibrin structure and functions," Journal of Thrombosis and Haemostasis. **vol**. **3**, no. 8, pp. 1894–1904(2005).
20. M. Mahmoodi et al., "Fabrication and Characterization of a Three-Dimensional Fibrin Gel Model to Evaluate Anti-Proliferative Effects of Astragalus hamosus Plant Extract on Breast Cancer Cells," Asian Pacific Journal of Cancer Prevention. **vol**. **23**, no. 2, pp. 731–741(2022).
21. F. Pourmorad, S. J. Hosseinimehr, and N. Shahabimajd, "Antioxidant activity, phenol and flavonoid contents of some selected Iranian medicinal plants," African journal of biotechnology. **vol**. **5**, no. 11(2006).
22. A. Shojaii, M. Motaghinejad, S. Norouzi, and M. Motevalian, "Evaluation of anti-inflammatory and analgesic activity of the extract and fractions of Astragalus hamosus in animal models," Iranian Journal of Pharmaceutical Research. **vol**. **14**, no. 1, pp. 263–269(2015).

Figures

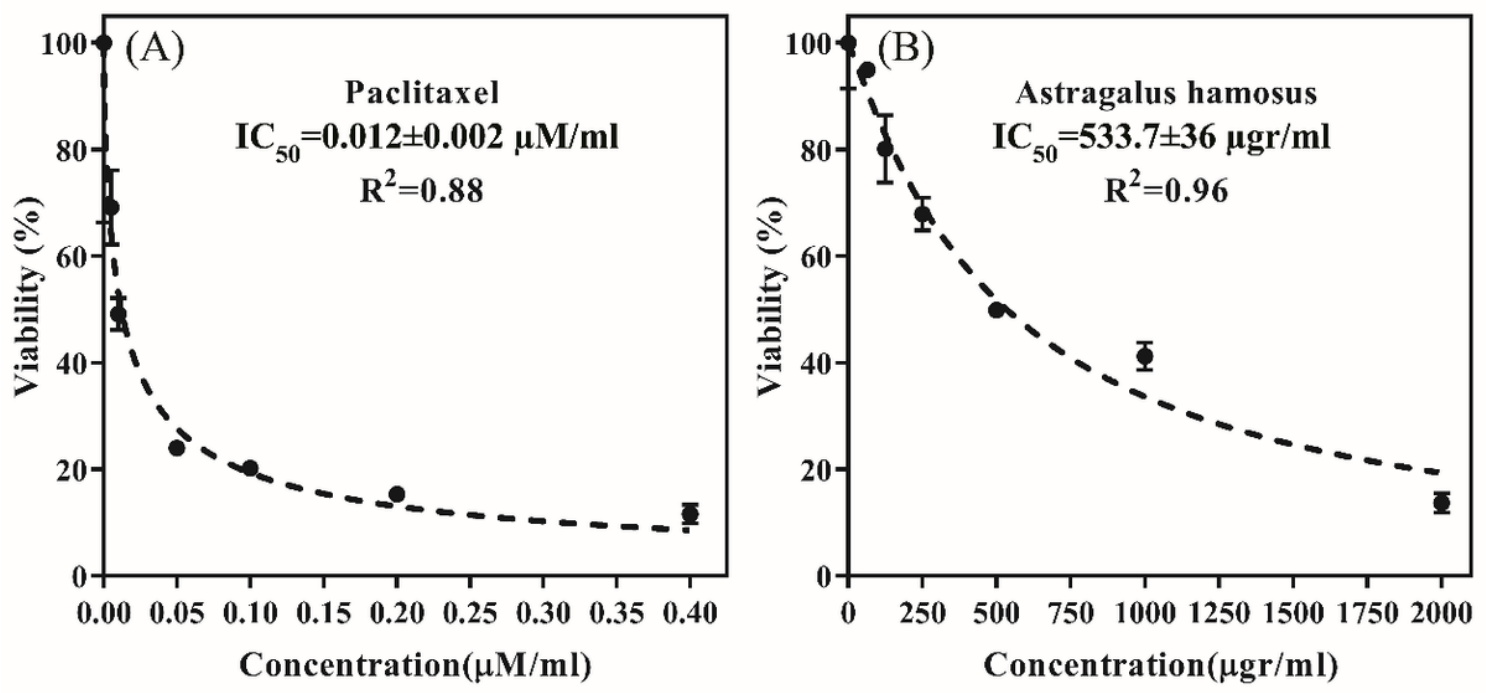

Figure 1

The IC_{50} of HUVEC Cells treated with various concentrations of (A) Paclitaxel and (B) *A. hamosus* in after 72 hours.

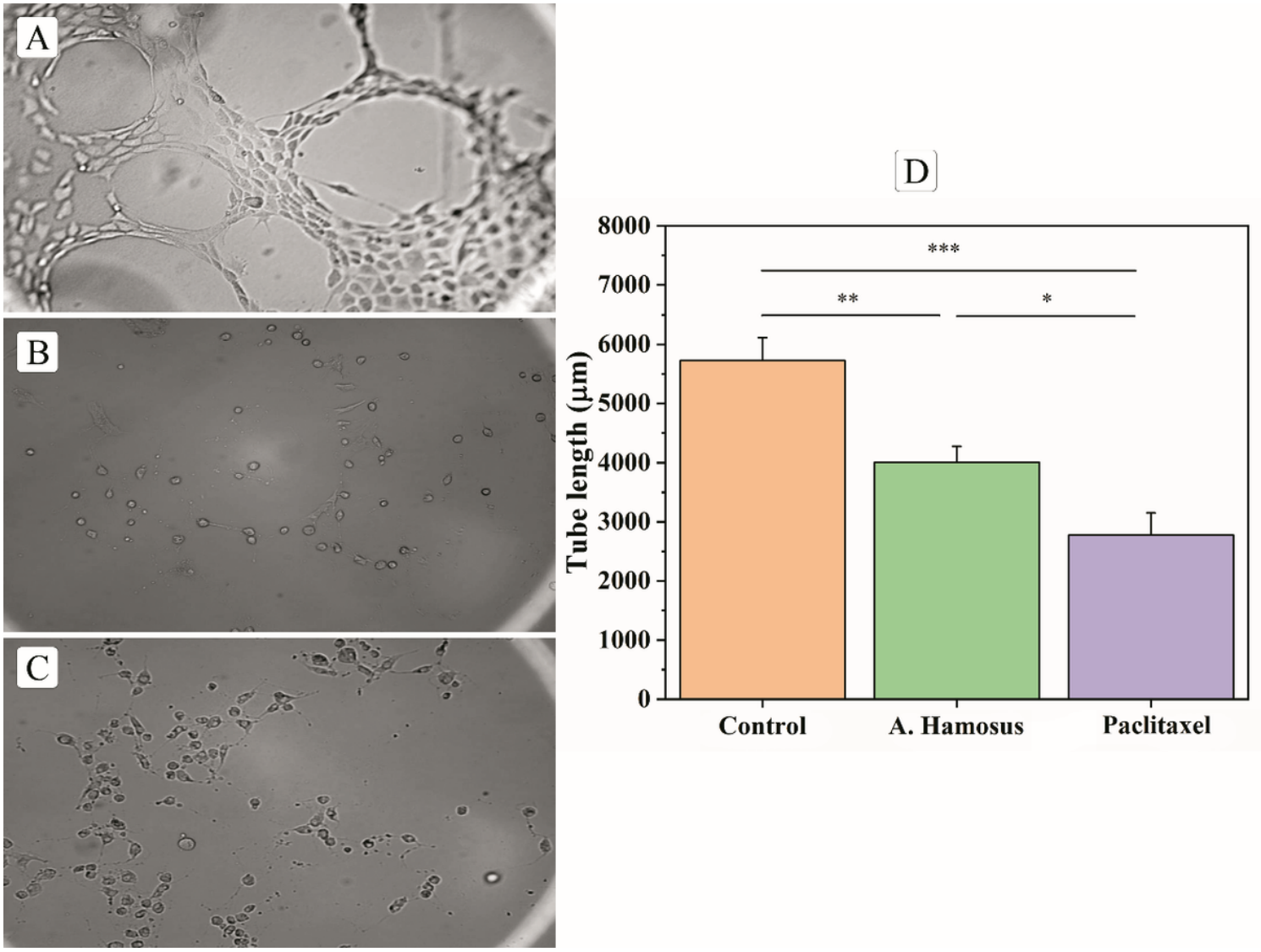

Figure 2

Tube formation of HUVEC cell line after 72 hours on (A) Negative control (untreated cells) (B) treated with Paclitaxel and (C) treated with *A. hamosus* extract. (D) The tube length of formed HUVEC tubes for experimental groups. Data show the means ± standard deviation. Different groups were compared statistically by One-way ANOVA (* $p<0.05$, ** $p<0.01$, *** $p<0.001$).

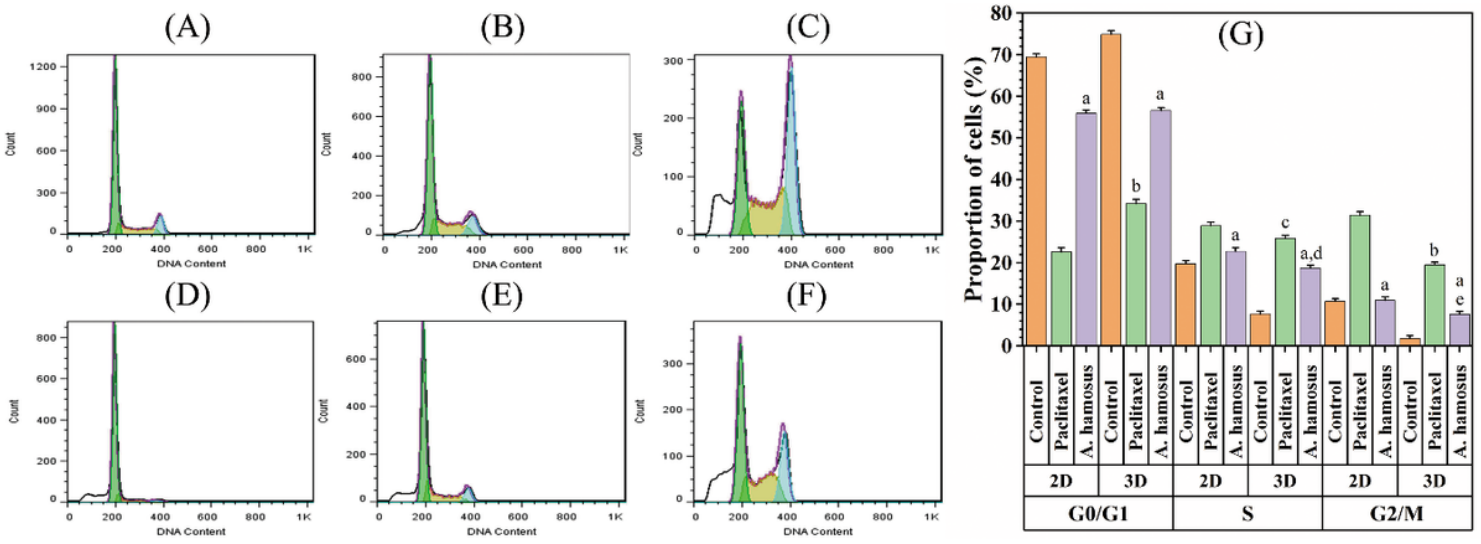

Figure 3

Cell cycle phases in HUVEC cells treated with IC_{50} concentrations of Paclitaxel and *A. hamosus* in 2D and 3D culture (A, B, and C: 2D untreated, PTX-, and *A. hamosus*-treated HUVECs; D, E, and F: 3D untreated, PTX-, and *A. hamosus*-treated HUVECs; G: percentage of cells in each cell cycle phase). Data show the means ± standard deviation. Different groups were compared statistically by One-way ANOVA (a: p<0.0001 (2D/3D) Paclitaxel-*A. hamosus*; b: p<0.0001 2D-3D Paclitaxel; c: p<0.01 2D-3D Paclitaxel; d: p<0.001 2D-3D *A. hamosus*; e: p<0.01 2D-3D *A. hamosus*).

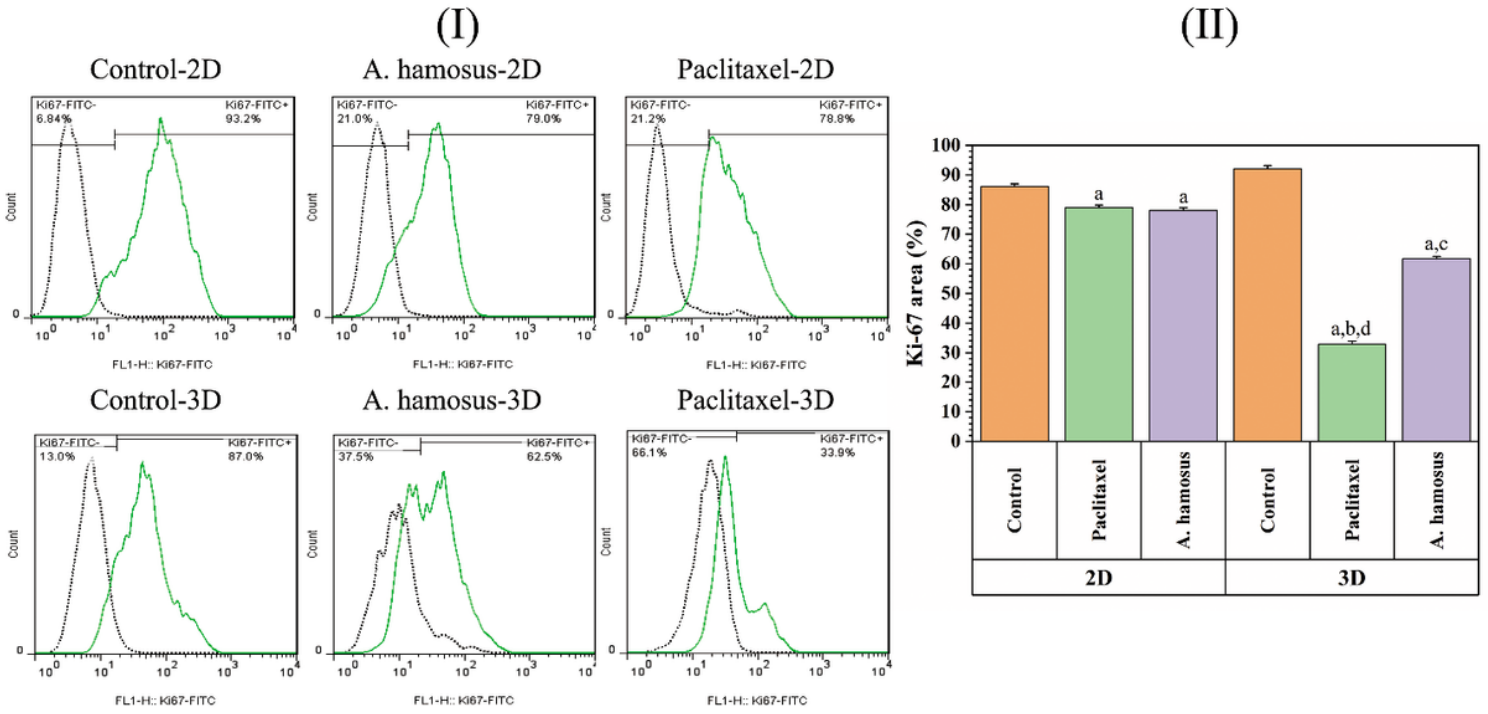

Figure 4

Percentage of Ki-67 expression in HUVEC cells treated with IC_{50} concentrations of Paclitaxel and *A. hamosus* in 2D and 3D culture. Data show the means ± standard deviation. Different groups were compared statistically by One-way ANOVA (a: p<0.0001 (2D/3D) Paclitaxel and *A. hamosus* compared to (2D/3D) Control; b: p<0.0001 2D-3D Paclitaxel; c: p<0.0001 2D-3D *A. hamosus*; d: p<0.0001 3D Paclitaxel-*A. hamosus*)

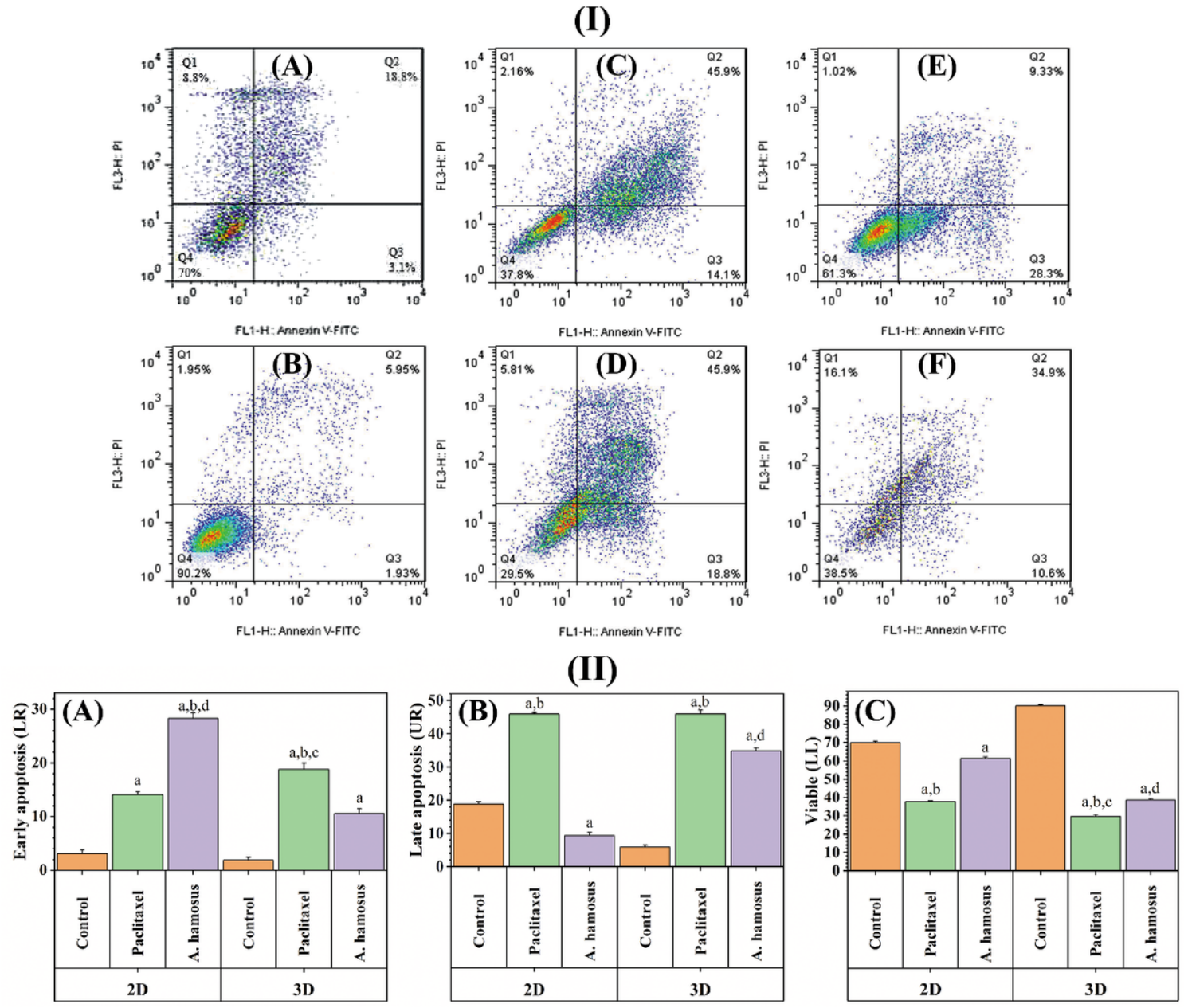

Figure 5

(I) Cell apoptosis by flow cytometry analysis of HUVEC cells treated with IC_{50} concentrations of Paclitaxel and *A. hamosus* in 2D and 3D culture. (A, C, E: Control, paclitaxel-, and *A. hamosus*-treated in 2D culture and B, D, F: Control, paclitaxel-, and *A. hamosus*-treated in 3D culture). (II) (A) Early apoptotic cells (B)

Late apoptotic cells (C) viable intact cells. Data show the means ± standard deviation. Different groups were compared statistically by One-way ANOVA (a: p<0.0001 (2D/3D) Paclitaxel and *A. hamosus* compared to (2D/3D) Control; b: p<0.0001 (2D/3D) Paclitaxel-*A. hamosus*; c: p<0.0001 2D-3D Paclitaxel; d: p<0.0001 2D-3D *A. hamosus*)

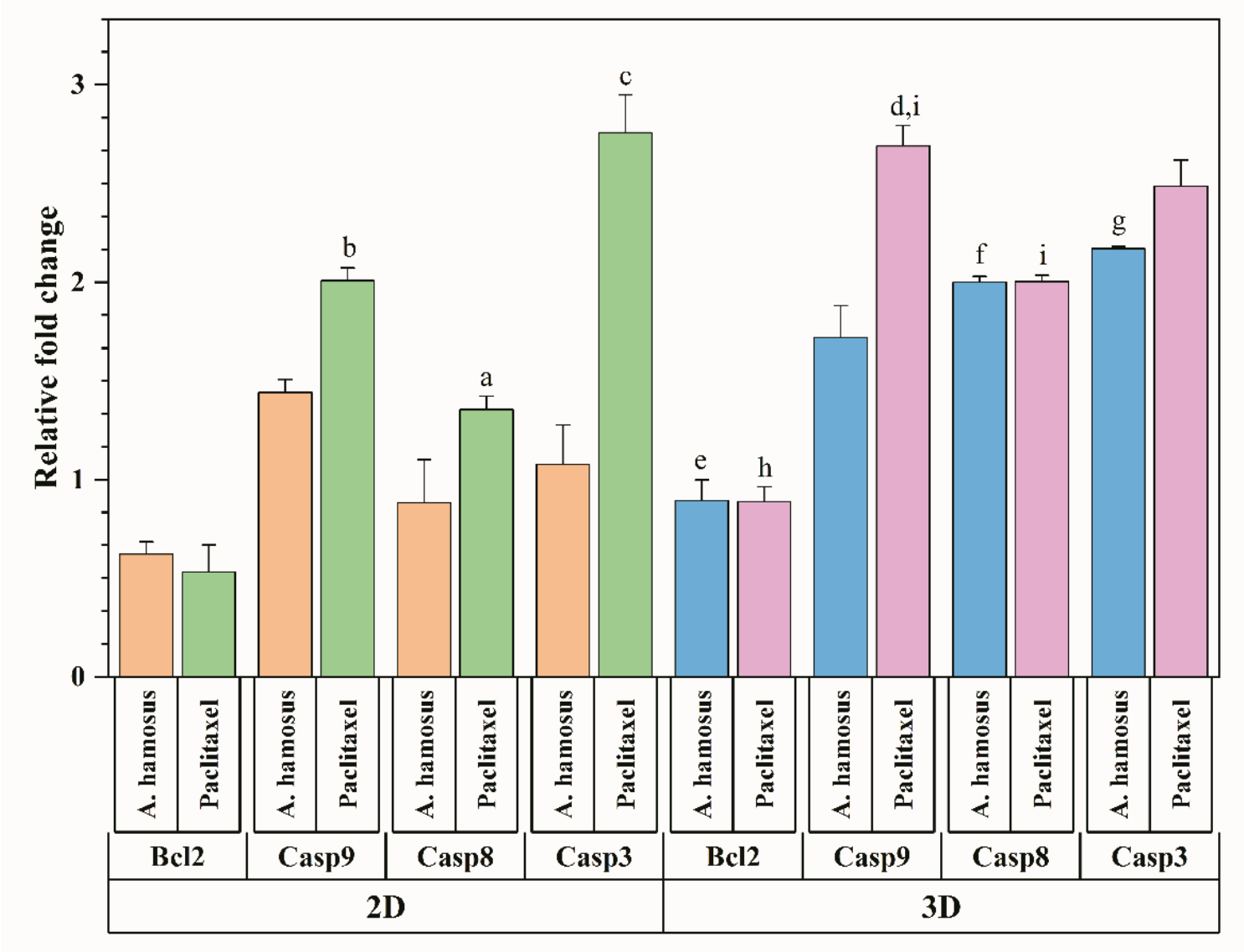

Figure 6

The result of mRNA expression for Pro-Apoptotic Genes (caspase-3, -8 and -9) and Anti-Apoptotic Gen Bcl-2 in HUVEC cells treated with *A. hamosus* and paclitaxel at the IC_{50} concentrations in 2D and 3D culture and normalized with β-globin as a house keeping gene. Data show the means ± standard deviation. Different groups were compared statistically by One-way ANOVA (a: p<0.01 2D Paclitaxel-*A. hamosus*; b: p<0.001 2D Paclitaxel-*A. hamosus*; c: p<0.0001 2D Paclitaxel-*A. hamosus*; d: p<0.0001 3D Paclitaxel-*A. hamosus*; e: p<0.05 2D-3D *A. hamosus*; f: p<0.0001 2D-3D *A. hamosus*; e: p<0.001 2D-3D *A. hamosus*; h: p<0.01 2D-3D Paclitaxel; i: p<0.001 2D-3D Paclitaxel).